Acta Cryst. (1993). B49, 605–610

Defect Structure and Diffuse Scattering of Zirconia Single Crystals with 10 and 15 mol% CaO at Temperatures up to 1750 K

BY TH. PROFFEN, R. B. NEDER AND F. FREY

Institut für Kristallographie und Mineralogie, Theresienstrasse 41, 8000 *München* 2, *Germany*

D. A. KEEN

ISIS Science Division, RAL, Didcot, Oxon, England

AND C. M. E. ZEYEN

ILL, BP 156, 38042 *Grenoble CEDEX* 9, *France*

(*Received* 21 *September* 1992; *accepted* 4 *January* 1993)

Abstract

Disorder diffuse scattering of CaO-stabilized zirconia was measured for two different CaO concentrations at temperatures up to 1750 K. There is no qualitative difference between the two samples at any temperature. Within the limits of an energy resolution of 0.1 THz, the diffuse scattering is of static origin. A quantitative interpretation is given in terms of two basic types of microdomains. Correlations exist along the ⟨111⟩ directions. The correlation lengths are independent of concentration and temperature, which only affect the relative amounts of uncorrelated to correlated microdomains. A pronounced change was observed at temperatures between 1150 and 1350 K. According to the published phase diagrams phase changes occur in this temperature regime. The diffuse scattering at very high temperatures seems to be in conflict with other interpretations based on precipitations of the $CaZr_4O_9$ (Φ_1) structure.

Introduction

Material properties of zirconia, ZrO_2, strongly depend on the specific defect and disorder structures which are affected by substitution by oxides like CaO, MgO, Y_2O_3. The disorder may be influenced by the kind of dopant, dopant concentration, temperature–time treatment, actual temperature and other factors. In consequence, the study of defect/disorder structures as a function of these parameters serves for a basic understanding of the physical properties of zirconia. In this paper we concentrate on the change of disorder with temperature in samples with different amounts of CaO.

At ambient pressure pure ZrO_2 possesses the cubic fluorite structure above 2643 K; on cooling it transforms into a distorted tetragonal fluorite phase and undergoes a transition into a monoclinic phase at temperatures around 1200–1300 K. By alloying with small amounts of CaO the phase boundaries are considerably changed, an intermediate ordered (Φ_1) phase $CaZr_4O_9$ occurring (*cf.* phase diagram by Hellmann & Stubican, 1983). Within the concentration limits 10–20 mol% CaO the cubic fluorite structure can be retained at room temperature (CSZ). Below 10 mol% CaO, down to approximately 6 mol%, single crystals show both cubic and tetragonal reflections. One should be aware, however, that the classification as 'cubic' zirconia concerns only the description of the *averaged* structure; averaging being done over the disorder elements. Discrepancies between different phase diagrams are probably related to the definition of real thermodynamically stable phases. For comparison, in MgO-stabilized zirconia (MgSZ) the analogous phase boundaries are shifted to higher temperatures. That means that the kinetics of the ordering processes are different, the same defect structures cannot be retained at lower temperatures. Precipitates of tetragonal ZrO_2 and a so-called δ-phase are reported to be responsible for diffuse scattering (Rossell & Hannink, 1984). In Y_2O_3-stabilized zirconia (YSZ) a local charge balance can be accomplished only by Y^{3+} diffusion or the defect cluster must have a net charge. Osborn *et al.* (1986) measured neutron diffuse scattering of YSZ up to 2200 K and found two components at the highest temperature, one of them being quasielastic. The other one can be interpreted in terms of a microdomain model based on paired oxygen vacancies. Therefore, it becomes clear why the defect structures in CSZ, MgSZ and YSZ may be different.

In CSZ with 15 and 7 mol% CaO the diffuse scattering was analysed successfully in terms of cor-

related microdomains (Neder, Frey & Schulz, 1990*a*,*b*; Proffen, Neder, Frey & Assmus, 1993). Rossell, Sellar & Wilson (1991) argue from electron microscopy (EM) observations that microdomains with the Φ_1 structure should be responsible for the diffuse scattering. An investigation of the temperature dependence of the diffuse scattering should shed some more light on this puzzle. The neutron method was chosen for two reasons: there are no absorption problems and the scattering power of the oxygens is comparable to that of the cations unlike in the X-ray method.

Experimental

Sample materials with nominal compositions $Zr_{0.9}Ca_{0.1}O_{1.9}$ and $Zr_{0.85}Ca_{0.15}O_{1.85}$ were supplied by W. Assmus, University of Frankfurt, Germany, and by Djevahirdjan Corporation, Switzerland, respectively. Both samples were transparent single crystals grown by the skull-melting technique with volumes of 0.7 and 1.3 cm^3, respectively. The former was found to consist of two crystallites with a volume of 3:7. They were intergrown with the [3 3 10] direction of the smaller one being parallel to [110] of the larger one. Fortunately the diffuse scattering of the two parts could clearly be separated (see below). The diffuse intensity was measured in sections either of the zeroth or the second layer of the [1$\bar{1}$0] zone.

The experiment with the 10 mol% CaO sample (CSZ10) was carried out at the time-of-flight instrument SXD at the neutron spallation source ISIS, RAL. A wavelength range between 0.25 and 8 Å could be used. The extended diffuse scattering was measured with a ZnS-scintillating position-sensitive detector with 16 × 16 elements providing an angular resolution $\Delta(2\theta) = 1.2°$. A furnace with vanadium heating elements (sample in vacuum) allowed measurements up to 1200 K. The collected data were corrected for the spectral distribution as determined by a vanadium scan, and for background scattering *via* an empty scan. The data were transformed into the momentum space by $Q = (m_n/h)(L)(2\sin\theta)(1/t)$ with L = flight distance, t = flight time, m_n = neutron mass, h = Planck's constant. At low Q, there are problems with a low monitor rate. Therefore, some uncertainties are unavoidable at low Q. To give an impression of the limits of confidence, error maps were drawn. Fig. 1 shows an example of the zeroth layer between the [110] and [111] directions measured at room temperature together with the corresponding error map.

The experiment with the 15 mol% CaO sample (CSZ15) was carried out using instrument D10 at the ILL, Grenoble, in the classical (triple-axis) diffractometer configuration: Cu(200) monochromator, PG(004) analyzer set in the elastic position, λ = 1.26 Å (very low high-order contamination at this wavelength). This experiment supplements earlier investigations with the same sample at higher temperatures. In selected areas of the second layer of the [1$\bar{1}$0] zone, pure elastic measurements were carried out with an energy resolution of 0.1 THz to separate diffuse parts of dynamic origin (Fig. 2). A mirror furnace developed by Lorenz (1988) and improved by Neder (1989) was used which operates under normal, *i.e.* oxidizing atmosphere and yields temperatures up to 2300 K.

Data evaluation and results

There are two basic features of the diffuse scattering of all the investigated zirconia samples: broad diffuse bands and diffuse maxima located around the positions of allowed Bragg reflexions. The superstructure wavevectors are $\pm(0.4\ 0.4\ \pm 0.8)$. As discussed in the next section the diffuse bands may be related to uncorrelated microdomains, whereas the diffuse peaks are due to correlated microdomains. Two different types of domains are involved. To learn about their temperature behaviour, the diffuse maxima were fitted by asymmetric two-dimensional Gaussians. The local principal axes a, b are rotated with respect to the underlying crystallographic [1$\bar{1}$0] and [001] axes by an angle α. The asymmetry was achieved by splitting the Gaussians halfway and weighting the halfwidth parameters on both sides of the maximum by γ and γ^{-1} (clearly the symmetric

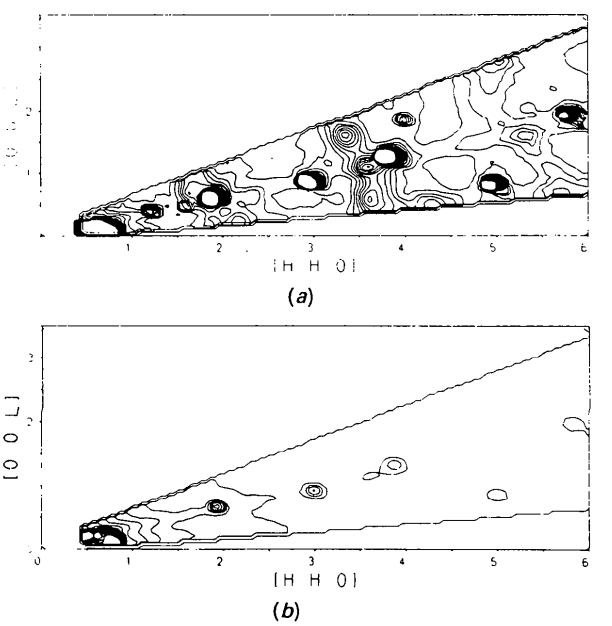

Fig. 1. Observed diffuse scattering of CSZ10 in the zeroth layer of the [1$\bar{1}$0] zone around the [111] direction (*a*) and corresponding error map (*b*).

case is denoted by $\gamma = 1$). Each diffuse maximum was therefore fitted by two parameters for the position, halfwidth parameters σ_a and σ_b, asymmetry parameters γ_a and γ_b, and one parameter for the integrated intensity. The angle α was kept fixed in either case. Some problems arose with the fitting of the broad diffuse bands. In the direction of the extension of the diffuse band there is only weak intensity variation. A two-dimensional Gaussian was used again with a very large extension along the band, the orientation of which was defined by an angle with respect to the [001] axis. The profile across the band was fitted by a Gaussian with three parameters (position, intensity, halfwidth) and by an additional constant background contribution. This procedure was not so straightforward in the case of the SXD data. Here an adequate weighting scheme had to be used after transforming from t into Q space, and the contamination of the diffuse scattering by the Bragg reflexions of the second crystallite was treated by excluded regions. Problems with fitting are unavoidable at the limits of these excluded regions. Only small sections of the zeroth layer of the [1 $\bar{1}$ 0] zone could be measured, and therefore no analysis of the diffuse bands could be carried out. Table 1 contains results for sample CSZ15, *viz.* integrated intensities and halfwidths of the diffuse maxima, the integrated intensity of the diffuse band, and a parameter describing an overall constant background. The peak positions were found to be equal to $\pm(0.4\ 0.4\ \pm 0.8)$ within the error limits; the asymmetry parameters γ fluctuate between 1.4 (1) and 1.6 (1) and around 1.1 (1) for both maxima, but do not show any significant temperature dependence. Table 2 contains corresponding values for sample CSZ10. In both cases a reliability factor R_{wp} gives a rough idea of the quality of the fits. This check can also be performed by inspection of Figs. 2 and 3. The left-hand columns show contour plots arising from the observed (corrected) data, the middle columns show the result of the calculations, and the right-hand columns show difference plots. Fig. 4 shows the temperature dependence of the integrated intensities of the diffuse maxima. Two values from the work of Neder *et al.* (1990*b*) are added. Note that squares and triangles refer to elastic measurements of the maximum at (2.8 1.6 3.6) of CSZ15 and crosses indicate the integrated measurement of the maximum (3.4 3.4 1.8) of CSZ10. In Fig. 5 the temperature evolution of the integral intensity of the diffuse band is plotted.

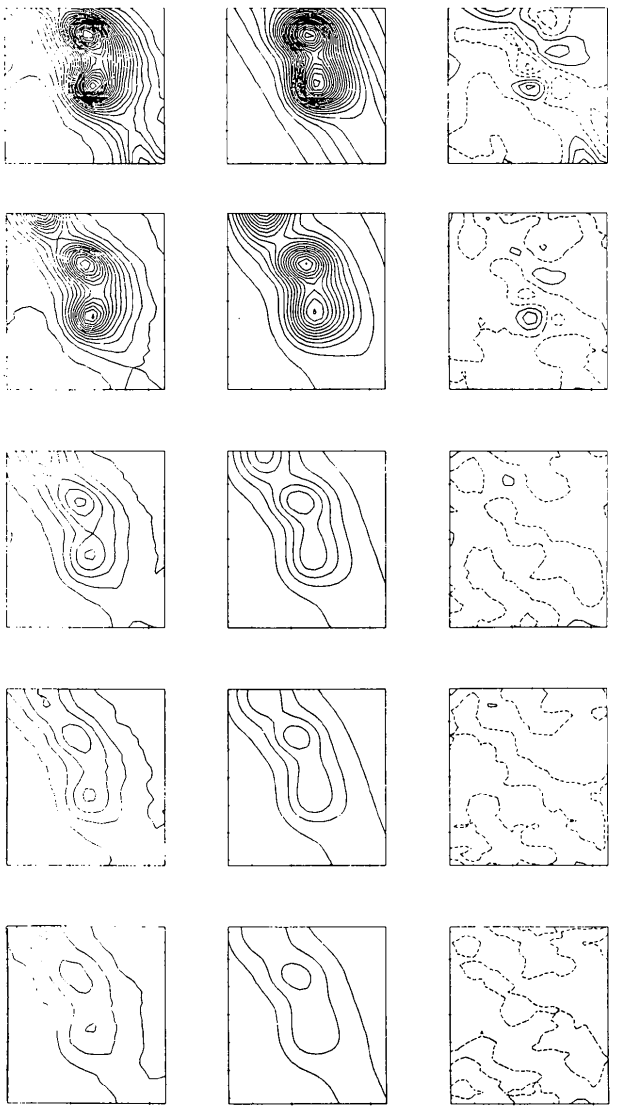

Fig. 2. Contour plots of the diffuse maxima (2.8 1.6 3.6) and (3.2 1.6 3.6) of CSZ15 measured at room temperature, 1150, 1350, 1550 and 1750 K (rows from above). Left, middle and right columns show observed, calculated and difference plots, respectively.

There is one unusual feature of the CSZ10 (SXD) data which can be seen immediately from Fig. 4: the data point at 823 K lies off the general tendency. Note that this temperature point was the last measured in the series room temperature, 998, 1203, 823 K. This will be discussed further in the next section.

Discussion

For CSZ15 it was shown in the work by Neder *et al.* (1990*b*) that the diffuse intensity can be described well by two types of microdomains. One type (*A*) is characterized by a single oxygen vacancy paired with one Ca ion at $\langle \frac{1}{4}+\delta\ \frac{1}{4}+\delta\ \frac{1}{4}+\delta \rangle$ and with relaxed nearest-neighbour positions. A second type (*B*) arises as a result of two oxygen vacancies spaced by $\langle \frac{1}{2}\ \frac{1}{2}\ \frac{1}{2} \rangle$,

Table 1. *Fit results of the data of CSZ*15 (*D*10)

	290 K	1150 K	1350 K	1550 K	1750 K
Diffuse peak at (2.8 1.6 3.6)					
I	26. (4.)	18. (2.)	7. (1.)	5.6 (9)	4.2 (9)
FW_a	0.227 (5)	0.257 (5)	0.247 (7)	0.259 (8)	0.27 (1)
FW_b	0.42 (2)	0.47 (2)	0.51 (3)	0.53 (3)	0.55 (4)
Diffuse peak at (3.2 1.6 3.6)					
I	14. (2.)	10. (1.)	3.6 (6)	2.6 (5)	2.1 (6)
FW_a	0.248 (8)	0.243 (7)	0.26 (1)	0.23 (1)	0.28 (2)
FW_b	0.25 (1)	0.26 (1)	0.27 (1)	0.28 (1)	0.31 (2)
Background and diffuse band (I_{DB})					
Back	44. (2.)	19. (1.)	15.5 (5)	12.6 (5)	12.7 (4)
I_{DB} ($\times 10^3$)	4.2 (3)	1.4 (1)	0.86 (8)	0.87 (8)	0.66 (6)
R_{wp} value					
R_{wp} (%)	16.6	18.3	17.7	18.4	18.9

Table 2. *Fit results of the data of CSZ*10 (*SXD*)

	290 K	823 K	998 K	1203 K
Diffuse peak at (3.4 3.4 1.8)				
I	0.05 (3)	0.02 (2)	0.03 (1)	0.02 (1)
FW_a	0.23 (4)	0.15 (4)	0.19 (3)	0.15 (3)
FW_b	0.26 (5)	0.20 (5)	0.25 (4)	0.21 (4)
Diffuse peak at (3.6 3.6 1.2)				
I	0.10 (5)	0.08 (5)	0.08 (3)	0.04 (2)
FW_a	0.43 (7)	0.44 (9)	0.43 (5)	0.41 (6)
FW_b	0.38 (7)	0.4 (2)	0.41 (6)	0.38 (6)
Diffuse peak at (3.6 3.6 0.8)				
I	0.10 (6)	0.03 (2)	0.05 (3)	0.02 (1)
FW_a	0.39 (7)	0.21 (6)	0.29 (4)	0.22 (4)
FW_b	0.4 (1)	0.3 (1)	0.4 (1)	0.32 (9)
Background				
Back	2.56 (6)	1.92 (5)	1.97 (3)	1.80 (3)
R_{wp} value				
R_{wp} (%)	33.9	37.8	23.9	23.2

one Ca ion between them, and again relaxed nearest-neighbour positions. In CSZ15 correlations were found to exist along ⟨111⟩ directions, but only between *A* and *A*, and *A* and *B*, but not between *B* and *B*. This model was also successful for interpretating the neutron diffuse scattering of CSZ7 (Proffen *et al.*, 1993). In particular it could be shown there that microdomains with tetragonal structure are not responsible for the diffuse scattering.

Recently EM observations of CSZ were interpreted in terms of microdomains with the Φ_1 structure (Rossell, Sellar & Wilson, 1991). This is in contrast with trial calculations of this structure using our model description of diffuse scattering (*cf.* Neder *et al.*, 1990*a*). The Φ_1 interpretation is also in conflict with the result of Cohen, Faber & Morinaga (1983) who state that calculated intensities do not agree with X-ray diffuse measurements for a sample with 13.4 mol% CaO. A further discussion is given by Proffen *et al.* (1993).

Generally we observe that the diffuse scattering is very similar for all CaO contents including a CSZ4 sample (not published): CSZ4, CSZ7, CSZ10, CSZ15. We conclude that the structures of the microdomains are largely unchanged irrespective of the CaO content. In other words, the kind of disorder is qualitatively the same in all CSZ samples as long as the averaged structure is the fluorite structure. Comparing CSZ15 with CSZ10, we also observe no major difference in the temperature behaviour of the disorder. In our interpretation, therefore, we have varying amounts of microdomains of both kinds, but no change of the basic structures of the domains nor a variation of the correlation lengths as a fraction of CaO concentration.

Neglecting for the moment the single point at 823 K (CSZ10, SXD), the integrated intensities of all diffuse scattering parts (maxima, band, background) become smaller with increasing temperature indicating a decrease of disorder (of any kind). This rules out a dynamic origin of disorder, a fact further supported by the absence of significant differences

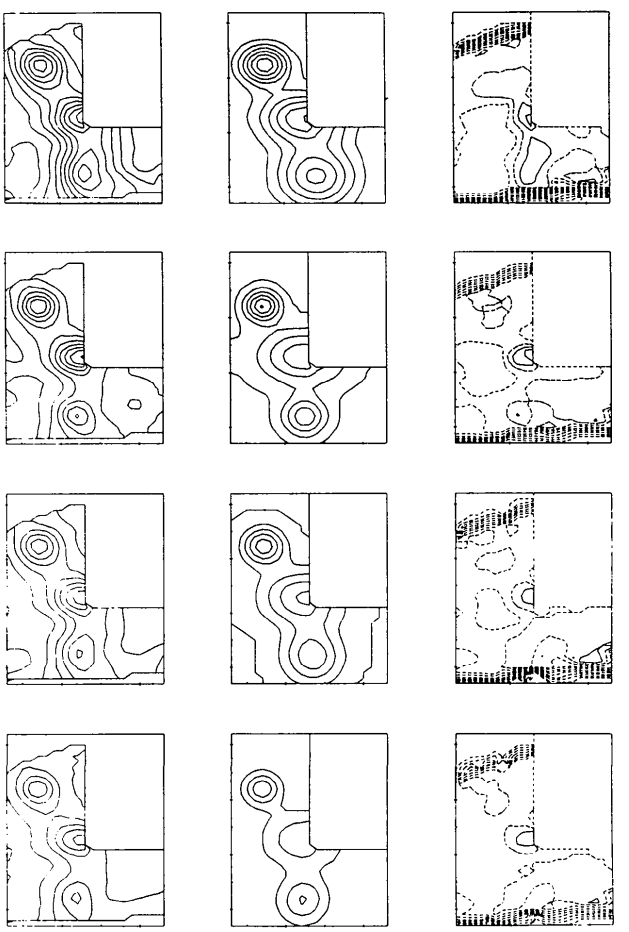

Fig. 3. Contour plots of the diffuse maxima (3.6 3.6 0.8), (3.6 3.6 1.2) and (3.4 3.4 1.8) of CSZ10 measured at room temperature, 833, 998 and 1203 K (rows from above). Left, middle and right columns show observed, calculated and difference plots, respectively.

between integral and elastic data. Because of the limited energy resolution, low frequency fluctuations might be responsible for (part of) the diffuse intensity. If so there would be, however, no remarkable increase of the frequency of this process exceeding the limits of our elastic energy window. This behaviour is different to that of YSZ where some of the diffuse scattering becomes quasielastic at temperatures as high as 2200 K (Osborn *et al.* 1986). Problems with the Φ_1 interpretation arise from the instability of this phase at temperatures above ~1500 K which is well below the temperature where diffuse scattering is still observable (*cf.* Figs. 2, 3). It was proposed by Rossell (1992) that Φ_1 microdomains should be forming and reforming dynamically at high temperatures. One would expect, however, a (critical?) increase of these fluctuations around the transition into the static domain behaviour. Correspondingly some anomalous increase of diffuse scattering should occur. We cannot confirm this idea from our data.

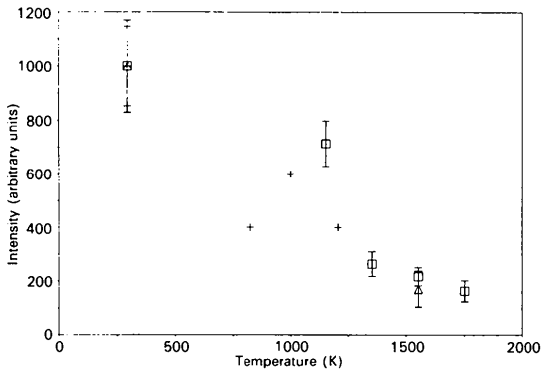

Fig. 4. *T*-dependence of the integrated intensity of diffuse maxima scaled to a common room-temperature value. Squares: CSZ15 (D10), crosses: CSZ10 (SXD), triangles: CSZ15 (taken from Neder *et al.* 1990*b*). Note that the single point at 823 K was measured upon cooling.

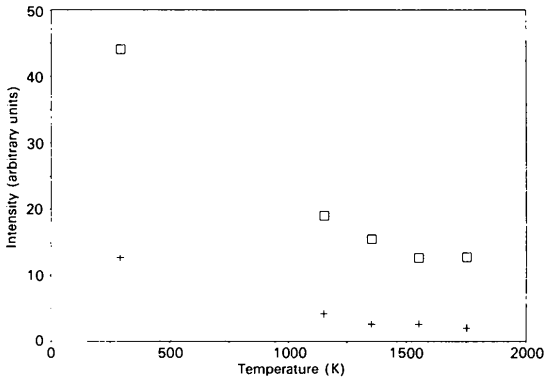

Fig. 5. *T*-dependence of the integrated intensity of the diffuse band (crosses) and of the diffuse background (squares). The error bars are within the size of the symbols.

Figs. 4 and 5 show that the integrated diffuse intensities of the maxima and of the diffuse band decrease with increasing temperature, but are still significant at the highest temperature of 1750 K that could be achieved in our experiment. The decrease of the intensity of the diffuse maxima is more pronounced between 1050 and 1350 K. From the phase diagram we know that this temperature interval corresponds to the temperature where the crystals enter the stability field of the fluorite structure. On the other hand, the halfwidths and shapes of the diffuse intensity concentrations are nearly unchanged. It may be concluded, therefore, that the amount of correlated microdomains decreases, whereas the correlation length remains unaffected. As mentioned, a considerable amount of diffuse scattering is still observable up to 1750 K, *i.e.* the disorder disappears only gradually. After cooling the diffuse scattering reappears without time delay which means that no remarkable activation energy exists for this order/disorder process. As observed by Marxreiter, Boysen, Frey, Schulz & Vogt (1990), however, the Φ_1 phase is only formed after annealing over several weeks. This again is not in favour of a Φ_1 explanation.

We relate the exceptional intensity behaviour of the diffuse peaks of CSZ10 at 823 K to the experimental conditions in the SXD experiment. As a result of the use of a vacuum furnace the sample underwent an irreversible change at high temperature, probably by reduction of the sample, shown by a change in the colour of the sample to light brown. This interpretation is further supported by the observations that other parts of the diffuse scattering also vanished after the sample had been heated up to 1203 K. In contrast to this result it should be emphasized that CSZ15 could be heated up to 1750 K in an oxidizing atmosphere without any permanent changes of the sample. However, this problem of oxidizing/reducing atmosphere demands further experimental investigations.

This work was supported by funds of the BMFT (grant No. 03-SC2LMU).

References

COHEN, J. B., FABER, J. JR & MORINAGA, M. (1981). *Advances in Ceramics*, Vol. 3, edited by A. H. HEUER & L. W. HOBBS, pp. 37–46. Columbus: American Ceramic Society.

HELLMANN, J. R. & STUBICAN, V. S. (1983). *J. Am. Ceram. Soc.* **60**, 260–264.

LORENZ, G. (1988). PhD thesis, Univ. München, Germany.

MARXREITER, J., BOYSEN, H., FREY, F., SCHULZ, H. & VOGT, T. (1990). *Mater. Res. Bull.* **25**, 435–442.

NEDER, R. (1989). PhD thesis, Univ. München, Germany.
NEDER, R., FREY, F. & SCHULZ, H. (1990*a*). *Acta Cryst.* A**46**, 792–798.
NEDER, R., FREY, F. & SCHULZ, H. (1990*b*). *Acta Cryst.* A**46**, 799–809.
OSBORN, R., ANDERSEN, N. H., CLAUSEN, K., HACKETT, M. A., HAYES, W., HUTCHINGS, M. T. & MACDONALD, J. E. (1986). *Mater. Sci. Forum.* **7**, 55–62.
PROFFEN, TH., NEDER, R. B., FREY, F. & ASSMUS, W. (1993). *Acta Cryst.* B**49**, 599–604.
ROSSELL, H. J. (1992). Personal communication.
ROSSELL, H. J. & HANNINK, R. H. J. (1984). *Advances in Ceramics*, Vol. 12, edited by N. CLAUSEN, H. HEUER & M. RÜHLE, pp. 139–151. Columbus: American Ceramic Society.
ROSSELL, H. J., SELLAR, J. R. & WILSON, I. J. (1991). *Acta Cryst.* B**47**, 862–870.

Acta Cryst. (1993). B**49**, 610–614

Structure of the Luminescent System Na^+/UO_2^{2+} β''-Alumina

BY MATS WOLF, ÅSA WENDSJÖ AND JOHN O. THOMAS

Institute of Chemistry, University of Uppsala, Box 531, *S*-751 21 *Uppsala, Sweden*

AND JAMES D. BARRIE

Department of Materials Science and Engineering, University of California, Los Angeles, CA 90024, *USA*

(*Received* 8 *October* 1992; *accepted* 25 *January* 1993)

Abstract

The structure and ionic distribution of Na^+ β''-alumina with ~12% of the sodium ions exchanged for the luminescent molecular uranyl ion (UO_2^{2+}) has been investigated at room temperature by single-crystal X-ray diffraction. The idealized formula for the crystal studied is $(UO_2)_y$-$Na_{1+x-2y}Mg_xAl_{11-x}O_{17}$, with $x = \frac{2}{3}$ and $y = 0.10$, $M_r = 627.8$. The structure has the trigonal space group $R\bar{3}m$, $a = 5.6206$ (3), $c = 33.703$ (5) Å, $V = 922.3$ (2) Å^3, $Z = 3$, $D_x = 3.39$ Mg m^{-3}, $\mu_{obs} = 2.03$, $\mu_{calc} = 2.30$ mm^{-1}. Spinel-type blocks comprising Al^{3+} ions, tetrahedrally and octahedrally coordinated by O^{2-} ions, are separated at $z = \frac{1}{6}, \frac{1}{2}$ and $\frac{5}{6}$ by conduction planes containing Na^+ and UO_2^{2+} ions and the column O atoms, O(5). These serve to hold together the spinel blocks through Al—O(5)—Al bonds. The Mg^{2+} ions stabilize the structure by substituting for one third of the Al^{3+} ions at Al(2) sites close to the centre of the spinel block ($z \simeq 0$). The linear UO_2^{2+} ions (length ~3.4 Å) arrange themselves in a disordered manner in the almost two-dimensional honeycomb-shaped pathways in the conduction planes, such that the molecules straddle the 6(*c*)-site intersections of the pathways. The uranium atoms occupy 18(*h*) sites, close to the Beevers–Ross (BR) 6(*c*) site, and the two uranyl O atoms occupy general 36(*i*) sites. The sodium ions occupy either BR sites or 18(*h*) sites, relaxed towards adjacent BR sites. Final $R(F) = 0.0252$, $R(F^2) = 0.0371$, $wR(F^2) = 0.0407$ for refinement on 2833 reflections.

Introduction

Sodium β''-alumina is a solid electrolyte exhibiting an unique ion-exchange chemistry, whereby a large number of mono-, di- and trivalent cations, as well as some protonic molecular ion species can be incorporated into the conduction planes. Many of the resulting materials are of clear technological interest, the most fascinating, perhaps, being their potential use in solid-state optical devices (Dunn, Farrington & Thomas, 1989).

This almost universal ion-exchange capability is made possible through the open-layered structure of β''-alumina. Compact spinel-type blocks of Al^{3+} and O^{2-} ions are separated by Al—O(5)—Al bridging bonds. It is within the almost two-dimensional layers so formed that Na^+ ions are situated and the Na^+ mobility can occur. It is therefore into these open regions that the various ionic species exchange. Schematic representations of the structure, with its honeycomb-shaped conduction paths, are shown in Fig. 1. In Na^+ β''-alumina, sodium ions occupy, on average, five out of six of the so-called Beevers–Ross (BR) sites (see Fig. 1*b*). This situation, with both crystalline [spinel blocks and O(5)] and disordered 'liquid-like' regions (conduction planes), complicates the interpretation of the space- and time-averaged crystallographic picture obtained.

This paper presents a structural investigation of an Na^+ β''-alumina single crystal in which ~12% of the sodium ions have been substituted for uranyl ions, UO_2^{2+}. These are molecular ions possessing a